Materials Science-Poland, *Vol.* 25, *No. 3, 2007*

Crystallization kinetics of SiO_2–MgO–3CaO–P_2O_5–Al_2O_3–ZrO_2 glass

S. YILMAZ[1*], V. GUNAY[2]

[1]Sakarya University, Engineering Faculty, Department of Metallurgy and Material Engeneering, Esentepe Campus, 54187 Sakarya, Turkey

[2]TUBITAK, MRC, Materials Institute, P.O Box 21, 41470 Gebze-Kocaeli, Turkey

The crystallization behaviour of SiO_2–MgO–3CaO–P_2O_5–Al_2O_3–ZrO_2 glass was studied using glass samples prepared by melting reagent grade SiO_2, MgO, $Ca_5(PO_4)_3OH$, P_2O_5, Al_2O_3 and ZrO_2. DTA and XRD analysis revealed the crystallization of whitlockite, anorthite and baddeleyite phases. The crystallization kinetics was studied by applying the DTA measurements carried out at various heating rates. The activation energies of crystallization and viscous flow were measured as 209 kJ·mol^{-1} and 356 kJ·mol^{-1}, respectively. The resultant SiO_2–MgO–3CaO–P_2O_5–Al_2O_3–ZrO_2 glass-ceramics revealed very fine and homogenous microstructure.

Key words: *bioceramics; bioglass; heat treatment; crystallization; kinetics*

1. Introduction

Ceramics used for the repair and reconstruction of diseased or damaged parts of the muscular-skelatal system, termed bioceramics, may be bioinert (alumina, zirconia), resorbable (tricalcium phosphate), bioactive (hydroxyapatite, bioactive glasses and glass-ceramics), or porous for tissue ingrowth (hydroxyapatite-coated metals, alumina). Bioceramics are needed to alleviate pain and restore function to diseased or damaged parts of the body [1, 2].

Ceramics and glasses are frequently used as biomaterials for the repair of bone tissue. They are popular because of their biocompatibility and the ability of firm composition into established bone. This latter property is described as bioactivity or osteoconductivity [3]. Natural bone and teeth are multiphase materials; their combination of properties probably can be simulated only by multiphase materials. Crystallization of glasses seems to be a very effective way to simulate hard tissues for those applications where elastic modulus mismatch and toughness are not important [4].

[*]Corresponding author, e-mail: symaz@sakarya.edu.tr

The first studies on glass-ceramics of the SiO_2–CaO–P_2O_5–MgO system were made by Kokubo and co-workers [5, 6]. Glass-ceramics can form a tight chemical bond with bones resulting in a high mechanical strength [7]. Moreover, after heat treatment, fine crystals such as apatite, wollastonite, whitlockite and Mg silicates precipitate from the glass matrix [7, 8] and they were found to have potential as biomaterials [8]. The crystals can enhance the mechanical strength and even promote the bioactivity of the glass-ceramics. Owing to such properties, the glass-ceramics in the SiO_2–CaO–P_2O_5–MgO system is used in clinic, either in the powder form as bone filler or in a bulk material for prosthetic application. The types of crystals formed in the glass matrix are determined by heat treatment and analyses of glass composition [8].

Kokubo, Lacerda, Salinas et al. [4–8] studied glass-ceramics of the SiO_2–CaO–P_2O_5 –MgO system based on comprehensive consideration of biological and medical properties. In this study, we studied the crystallization kinetics of SiO_2–MgO–CaO–P_2O_5–Al_2O_3–ZrO_2 glass system. Al_2O_3 and ZrO_2 were added to glass composition to improve some properties such as strength and chemical resistance of the glass-ceramic system [9, 10].

2. Experimental

The SiO_2–MgO–3CaO–P_2O_5–Al_2O_3–ZrO_2 glass was melted from reagent grade SiO_2, MgO, $Ca_5(PO_4)_3OH$, P_2O_5, Al_2O_3 and ZrO_2. The composition of the bioglass sample is given in Table 1.

Table 1. Glass composition

Compound	Content [wt. %]
SiO_2	40.00
CaO	14.00
MgO	10.00
P_2O_5	18.00
Al_2O_3	12.00
ZrO_2	6.00

The calculated batch was melted in platinum–2% rhodium crucible at 1500 °C for 2 h using an electric furnace (HERAEUS). To ensure homogeneity, the melt was poured into water. The cast was crushed, pulverised and remelted at the same temperature for 2 h and rotated several times in 30 min intervals to achieve homogeneity. The refined and homogenized melt was cast into a preheated stainless steel rectangular mould with the dimensions (1×3×0.5 cm^3). In order to remove thermal residual stress of the glass sample, it was annealed in a regulated muffle furnace at about 600 °C for 1 h. The muffle furnace was left to cool to room temperature at the rate of 30 °C·h^{-1}. Glass-ceramic samples were prepared by applying suitable heat treatments planned

according to the results of differential thermal analysis (DTA) of the amorphous glass. Heat treatments were carried out at temperatures of 800, 900 and 1000 °C for 1 h in a Lenton tube furnace to promote internal crystallization. The crystallization temperatures were selected from the DTA curve depending on the endothermic and exothermic reaction temperatures (Table 1). The crystallization kinetics was studied by the differential thermal analysis (DTA) to determine the activation energies for the crystallization and the viscous flow. The crystalline phase in the heat treated glass samples was determined by X-ray diffraction (XRD) analysis using a RIGAKU D/MAX-2200/PC diffractometer using CuK_α radiation (1.5418 Å). The kinetics of crystallization of glass was determined by the DTA experiments performed in a Netzch STA 429 thermoanalyser using 200 mg powdered samples and employing heating rates of 5, 10, 15 and 20 °C·min^{-1} in open atmosphere with Al_2O_3 powder as a reference material. Some of the crystallized glass specimens were mounted in conductive resin, ground with 600, 1200 and 2500 grit of silicon carbide and finally polished with 1 μm diamond slurry to observe microstructure using a JEOL 6060 LV scanning electron microscope (SEM).

3. Results and discussion

3.1. Differential thermal analysis and crystalline phases

The DTA curves of the glasses are presented in Fig. 1. Endothermic reactions at the temperature range of 665–691 °C have been identified. These endothermic peaks are attributed to the glass transition (T_g), at which the sample changes from solid to liquid behaviour. Various exothermic effects such as that at 734–762 °C indicating reaction of crystallization in the glasses are also recorded.

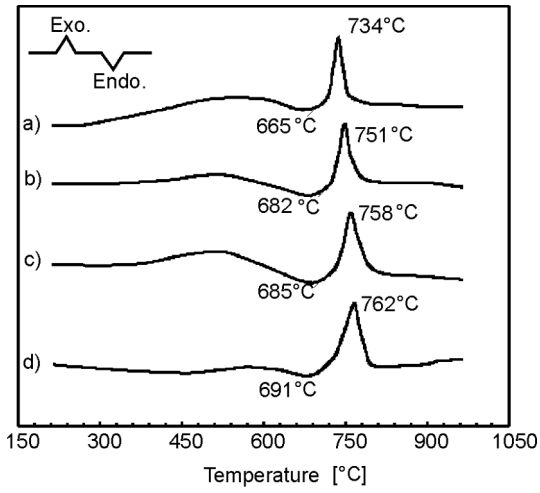

Fig. 1. DTA diagrams of the SiO_2–MgO –3CaO–P_2O_5–Al_2O_3–ZrO_2 glass at the heating rates of: a) 5 °C/min, b) 10 °C/min, c) 15 °C/min and d) 20 °C/min

The appearance of a crystallization peak on the DTA curve implies that at least a different crystal phase is formed during the heat treatment. This was also confirmed by XRD results (Fig. 2). This agrees with previous studies [11, 12].

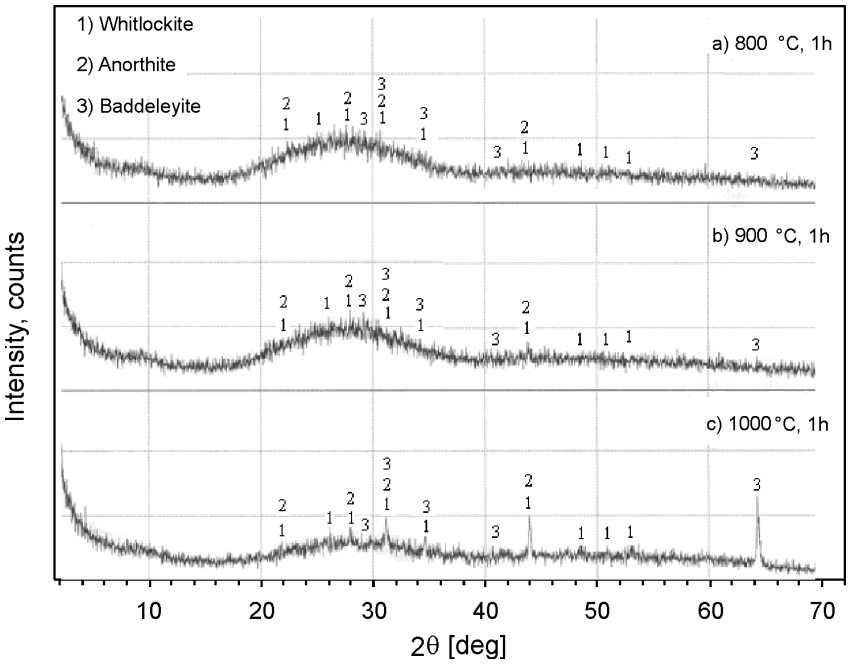

Fig. 2. X-ray diffraction patterns of the SiO_2–MgO–3CaO–P_2O_5–Al_2O_3–ZrO_2 glass-ceramics heat treated at 800, 900 and 1000 °C for 1 h

The XRD analysis of bioglass sample showed no crystalline peaks. The cast and annealed glass structure was amorphous and so the spontaneous cooling obtained by glass melt in the furnace ensures glass formation. Figure 2 shows the resulys of XRD analysis of glass samples heat treated at 800, 900 and 1000 °C for 1 h. The determined crystal phase was whitlockite ($Ca_3(PO_4)_2$) (card number: PDF 09-0169), anorthite ($2CaAl_2Si_2O_8$) (card number: PDF 01-070-0287) and baddeleyite (ZrO_2) (card number: PDF 01-072-1669). The degree of crystallization is low in the bioglass-ceramics heat treated at 800 and 900 °C for 1 h (Fig. 2a, b), peaks are not visible clearly and the sample seems to be nearly amorphous. The bioglass system started to crystallize but the ratio of crystallization was not high enough for complete transformation of glass-ceramics. This may be due to high Al_2O_3 content in glass composition leading to inhibition of crystallization [13]. The maximum crystallization was observed in the bioglass-ceramics heat treated at 1000 °C for 1 h (Fig. 2c). XRD analysis showed that the higher is the crystallization temperature the higher the whitlockite peak. Increase in treatment temperature leads to the formation of higher amounts of crystalline phase [11, 12].

3.2. Microstructure

SEM micrograph of the polished surface of the glass-ceramics is shown in Fig. 3.

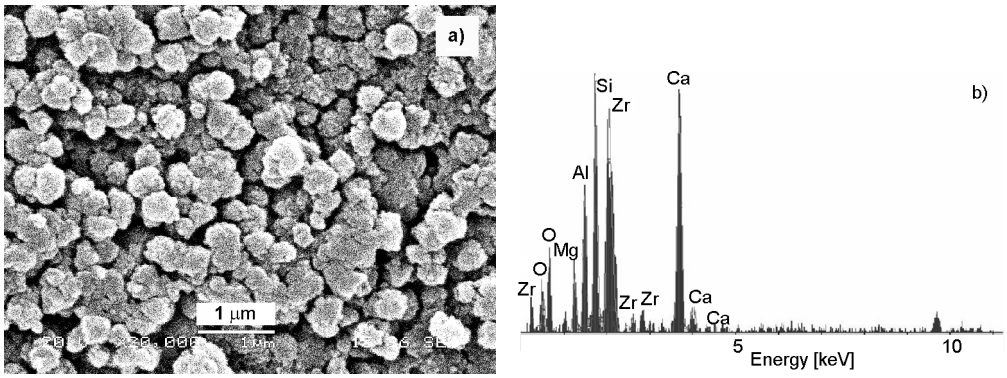

Fig. 3. SEM micrograph (a) and EDAX spectrum (b) of the surface of the glass-ceramic specimen heat treated at 1000 °C for 1 h and etched using 2.5 % HF in ethanol for 30 s

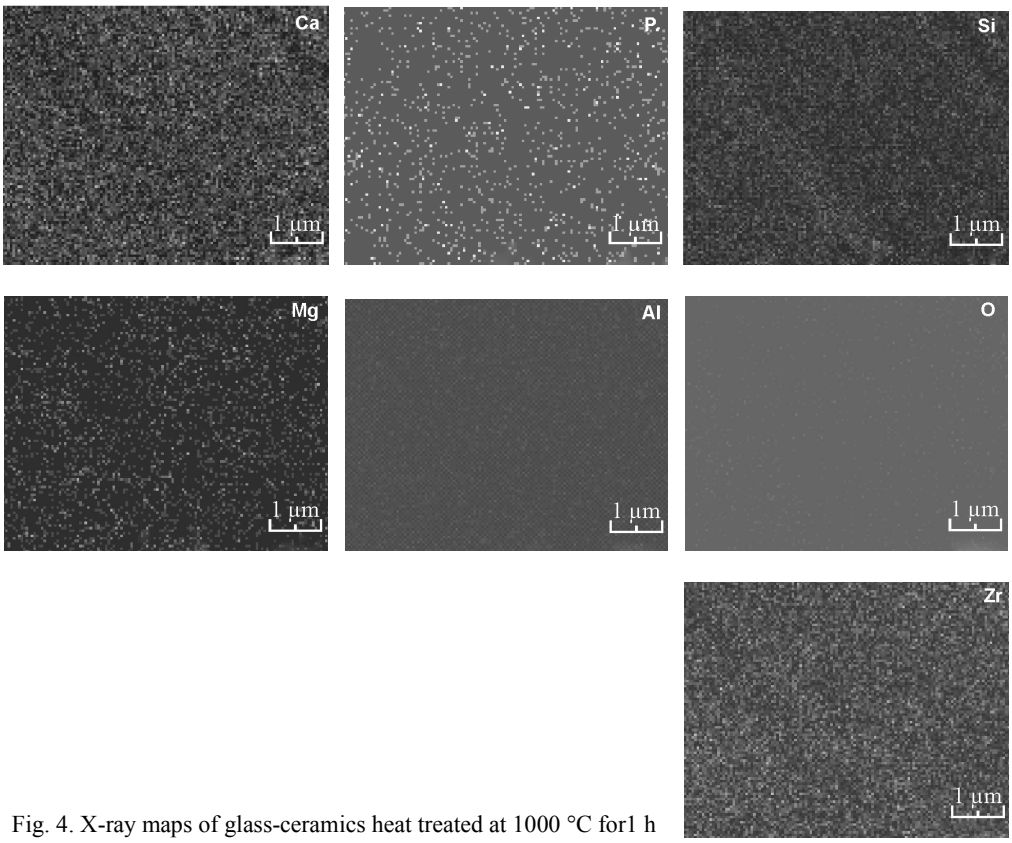

Fig. 4. X-ray maps of glass-ceramics heat treated at 1000 °C for1 h

Glass microstructure of samples heat treated at 1000 °C is not clear: whitlockite, anorthite and baddeleyite crystals detected by XRD are very small (< 1 μm). The highest peak belongs to Si and Ca in the EDAX analysis (Fig. 3b); whitlockite, anorthite and baddeleyite crystals are present in the glassy matrix. From the amorhous glassy matrix, Ca, P, Al, Si and Zr leave to crystallize in whitlockite, anorthite and baddeleyite phases. This was also confirmed by XRD results (Fig. 2). In Figure 4, X-ray maps of the glass-ceramics heat treated at 1000 °C 1 h are shown. All elements are homogenously distributed in the sample.

3.2. The kinetics of crystallization

Solid state reactions such as crystallization of glass can be described by the phenomenological Johnson–Mehl–Avrami (JMA) equation [11, 12, 14].

$$X = 1 - \exp\left[-(kt)^n\right] \tag{1}$$

Taking natural logarithms and rearranging Eq. (1), we obtain

$$\ln(1 - X) = n \ln k + n \ln t \tag{2}$$

where X is the volume fraction crystallized after time t [11, 12, 14], n is the Avrami parameter which depends on the growth direction number and the mechanism of nucleation and crystal growth [11, 12, 15] shown in Table 2, and k is the reaction rate constant [s^{-1}] whose temperature dependence being expressed by the Arrhenius equation:

$$k = V \exp\left(-E_a/RT\right) \tag{3}$$

where V is the frequency factor [s^{-1}], E_a – the activation energy for crystallization [$J \cdot mol^{-1}$], R – the gas constant and T – the absolute temperature [K] [11, 12].

Table 2. Values of the parameter n for various crystallization mechanisms [11, 12]

Mechanism	n
Bulk nucleation	
Three-dimensional growth	4
Two-dimensional growth	3
One-dimensional growth	2
Surface nucleation	1

From the value of the activation energy E_a, the Avrami parameter n can be calculate by the DTA results [11, 12, 16]:

$$n = \frac{2.5}{\Delta T}\frac{T_p^2}{(E_a/R)} \tag{4}$$

where ΔT is the full width of the exotermic peak at the half maximum intensity from DTA crystallization peak. The value of the activation energy for crystallization of glasses was determined using a method based on JMA equation which was first introduced by Kissenger and modified by others. This method is based on the dependence of the crystallization peak temperature (T_p) on the DTA heating rate (β) [10, 12, 15–17]:

$$\ln\frac{T_p^2}{\beta} = \ln\frac{E_a}{R} - \ln V_a + \frac{E_a}{RT_p} \tag{5}$$

likewise, Eq. (5) can also be used to predict the viscous energy [11, 12]:

$$\ln\frac{T_g^2}{\beta} = \ln\frac{E_c}{R} - \ln V_c + \frac{E_c}{RT_g} \tag{6}$$

where E_c is the corresponding activation energy for viscous flow, T_g is the glass transformation temperature, V_a is the frequency factor for crystallization and V_c is the frequency factor for viscous flow.

Plots of $\ln(T_p^2/\beta)$ vs. $1/T_p$ and $\ln(T_g^2/\beta)$ vs. $1/T_g$ obtained at various heating rates should be linear with the slopes E_a/R and the intercepts $\ln(E_a/R) - \ln V_a$ and $\ln(E_c/R) - \ln V_c$. Therefore, if E_a/R and E_c/R are estimated from the slope, the frequency factors can be calculated from the intercepts [11, 12]. The peak temperatures (T_g and T_p) changing with heating rates and T values for calculating n are given in Table 3. The same data are plotted in Figs. 5 and 6.

Table 3. The results of DTA for SiO_2–MgO–3CaO–P_2O_5–Al_2O_3–ZrO_2 glass

Heating rate, β [K·min^{-1}]	Peak temperature [°C]		ΔT [°C]
	T_g	T_p	
5	665	734	17
10	682	751	25
15	685	758	26
20	691	762	28

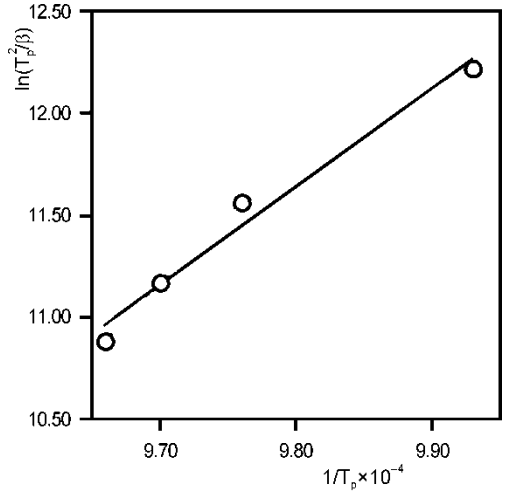

Fig. 5. Plot of ln T_p^2/β vs. $1/T_p$ for the determination of the activation energy for the crystallization of SiO_2–MgO–3CaO–P_2O_5–Al_2O_3–ZrO_2 glass

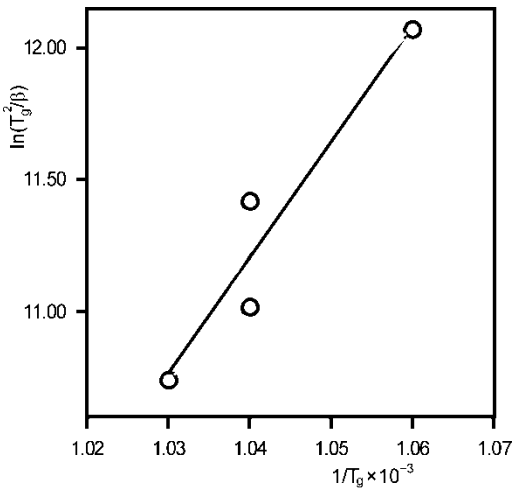

Fig. 6. Plot of ln T_g^2/β versus $1/T_g$ for the determination of the activation energy for the viscous flow of SiO_2–MgO–3CaO–P_2O_5–Al_2O_3–ZrO_2 glass

In accordance with the literature data, the temperature corresponding to the crystallization peak is higher at faster heating rates [11]. The calculated values of E_a, E_c and V_a,V_c (Figs. 6 and 7) are as follows: E_a = 209 kJ·mol^{-1}, E_c = 356 kJ·mol^{-1}, $V_a = 2.37\times 10^{10}$ s^{-1}, $V_c = 3.91\times 10^{10}$ s^{-1}.

Table 4. The n values of SiO_2–MgO–3CaO–P_2O_5–Al_2O_3–ZrO_2 glasses

Heating rate, β [K·min^{-1}]	5	10	15	20
n	4.0	4.1	4.0	3.7

The n values, calculated from Eq. (4), are given in Table 4. It can be seen that $n \cong 4$ and $n > 4$, which indicates that the crystallization of the SiO_2–MgO–3CaO –P_2O_5–Al_2O_3–ZrO_2 glass at all heating rates is caused by bulk nucleation with three-dimensional crystal growth.

4. Conclusions

In the crystallization of the SiO_2–MgO–3CaO–P_2O_5–Al_2O_3–ZrO_2 glass, whitlockite ($Ca_3(PO_4)_2$) crystallizes. The Johnson–Mehl–Avrami, Kissenger and Mahadevan equations were used to calculate the activation energies of crystallization and of viscous flow. The dimensionless parameter n, related to the reaction mechanism was determined by using T values obtained from DTA measurements at various heating rates. Depending on the heating rate, the n values varied between 3.7 and 4.1, indicating the

bulk nucleation in the SiO_2–MgO–3CaO–P_2O_5–Al_2O_3–ZrO_2 glass by three-dimensional crystal growth. The activation energies of the crystallization and of viscous flow were calculated as 209 kJ mol^{-1} and 356 kJ mol^{-1}, respectively.

Acknowledgements

The authors would like to express their gratitude to Sakarya University Engineering Faculty and Prof. Dr. Cuma Bindal, the Head of the Department of Metallurgy and Materials Engineering for supporting this work. The authors are also grateful to Tarık Baykara, the Head of TUBITAK, MRC, Materials Institute, Turkey. The authors express their grateful thanks to technician Ersan Demir at Metallurgical and Material Engineering Laboratory of Sakarya University, Turkey and Müberra Yılmaz (MSc) for assisting with writing, checking and experimental assistance.

References

[1] HENCH L.L., J. Amer. Cer. Soc., 74 (1991), 1487.
[2] HENCH L.L., J. Amer. Cer. Soc., 81 (1998), 1705.
[3] SALAM S.N., DARWISH H., ABO-MOSALLAM H.A., Ceramics Int., 32 (2006), 357.
[4] SALINAS A.J., ROMAN J., VALLET-REGI M., OLIVEIRA J.M., CORREIA R.N., FERNANDES M.H., Biomater., 21 (2000), 251.
[5] KOKUBO T., Biomater., 12 (1991), 155.
[6] KOKUBO T., ITO S., SAKKA S., YAMAMURO T., J. Mater. Sci., 21 (1986), 536.
[7] CHANG C.K., MAO D.L., WU J.S., Ceramics Int., 26 (2000), 779.
[8] LACERDA S.R., OLIVEIRA J.M., CORRIERA R.N., FERNANDES M.H., J. Non-Cryst. Sol., 221 (1997) 255.
[9] DEMIRKESEN E., MAYTALMAN E., Ceramics Int., 27 (2001), 99.
[10] DEMIRKESEN E, GOLLER G., Ceramics Int., 29 (2003), 463.
[11] YILMAZ S., OZKAN O.T., GUNAY V., Ceramics Int., 22 (1996), 477.
[12] BAYRAK G., YILMAZ S., Ceramics Int., 32 (2006), 441.
[13] MCMILLAN P.W., *Glass-ceramics*, 2nd Ed., Academic Press, London, 1979.
[14] BALAYA P., SUNANDANA C.S., J. Non-Cryst. Sol., 162 (1993), 253.
[15] KARAMANOV A., PELINO M., J. Non-Cryst. Sol., 281 (2001), 139.
[16] PARK J., HEO J., Ceramics Int., 28 (2002), 669.
[17] EROL M., KUCUKBAYRAK S., MERICBOYU A.E., OVECOGLU M.L., J. Europ. Cer. Soc., 21 (2001), 2835.

Received 21 June 2006
Revised 28 December 2006